

# Improved dispersion relations for $\gamma\gamma \rightarrow \pi^0\pi^0$

José A. Oller<sup>a</sup>, Luis Roca<sup>a</sup> and Carlos Schat<sup>a,b</sup>

<sup>a</sup>*Departamento de Física. Universidad de Murcia. E-30071, Murcia. Spain.*

<sup>b</sup>*CONICET and Departamento de Física, FCEyN, Universidad de Buenos Aires,  
Ciudad Universitaria, Pab.1, (1428) Buenos Aires, Argentina.*

*oller@um.es , luisroca@um.es , schat@df.uba.ar*

## Abstract

We perform a dispersive theoretical study of the reaction  $\gamma\gamma \rightarrow \pi^0\pi^0$  emphasizing the low energy region. The large source of theoretical uncertainty to calculate the  $\gamma\gamma \rightarrow \pi^0\pi^0$  total cross section for  $\sqrt{s} \gtrsim 0.5$  GeV within the dispersive approach is removed. This is accomplished by taking one more subtraction in the dispersion relations, where the extra subtraction constant is fixed by considering new low energy constraints, one of them further refined by taking into consideration the  $f_0(980)$  region. This allows us to make sharper predictions for the cross section for  $\sqrt{s} \lesssim 0.8$  GeV, below the onset of D-wave contributions. In this way, were new more precise data on  $\gamma\gamma \rightarrow \pi^0\pi^0$  available one might then distinguish between different parameterizations of the  $\pi\pi$  isoscalar S-wave. We also elaborate on the width of the  $\sigma$  resonance to  $\gamma\gamma$  and provide new values.

# 1 Introduction

The reaction  $\gamma\gamma \rightarrow \pi^0\pi^0$  measured in ref.[1] offers the interesting prospects of having a two-body hadronic final state and the important role of final state interactions in S-wave enhanced due to the null charge of the  $\pi^0$ . These two facts make this process very suited for learning about the non-trivial  $\pi\pi$  isospin ( $I$ ) 0 S-wave. In addition, it was taken as an especially appropriate ground test for Chiral Perturbation Theory ( $\chi$ PT) [2, 3], since at lowest order this process is zero and at next-to-leading order (one loop) is a prediction free of any counterterm [4, 5]. However, the one loop  $\chi$ PT prediction departs very rapidly from data just above the threshold and only the order of magnitude was rightly foreseen. A two loop calculation in ref.[6, 7] was then undertaken with better agreement with data [1]. The three counterterms that appear at  $\mathcal{O}(p^6)$  are fixed by the resonance saturation hypothesis. Other approaches supplying higher orders to one loop  $\chi$ PT by taking into account unitarity and analyticity followed [8, 9, 10]. Ref.[10] is a Unitary  $\chi$ PT calculation in production processes [10, 11, 12, 13, 14, 15] and was able to provide a good simultaneous description of  $\gamma\gamma \rightarrow \pi^0\pi^0$ ,  $\pi^+\pi^-$ ,  $\eta\pi^0$ ,  $K^+K^-$  and  $K^0\bar{K}^0$  from threshold up to rather high energies,  $s^{1/2} \lesssim 1.5$  GeV. This approach was also used in ref.[16] to study the  $\eta \rightarrow \pi^0\gamma\gamma$  decay.

We concentrate here on the dispersive method of refs.[17, 18, 19]. We critically review and extend it, so as we are able to drastically reduce the uncertainty due to the not-fixed phases above the  $K\bar{K}$  threshold of the  $I = 0$  S-wave  $\gamma\gamma \rightarrow \pi\pi$  amplitude. This is accomplished by using an  $I = 0$  S-wave Omnès function that is continuous under changes in the phase function employed for its evaluation above the  $K\bar{K}$  threshold. Equivalently, one can introduce an additional subtraction in the dispersion relation to evaluate the  $I = 0$  S-wave  $\gamma\gamma \rightarrow \pi\pi$  amplitude to those considered in ref.[17, 18, 19, 8]. This new subtraction constant is fixed by considering simultaneously three constraints instead of the two employed in the previous references. As a result of this much reduced uncertainty, the total cross section  $\sigma(\gamma\gamma \rightarrow \pi^0\pi^0)$  might be used to distinguish between different S-wave  $I = 0$  phase shift parameterizations once new more precise experimental data become available. We also perform calculations of the width  $\Gamma(\sigma \rightarrow \gamma\gamma)$ , taking from the literature different  $\sigma$  resonance parameters, and compare with the value of ref.[17]. Other papers dedicated to calculate the two photon decay widths of hadronic resonances are [20].

The content of the paper is as follows. In section 2 we discuss the dispersive method of ref.[18] and extend it to calculate with higher accuracy the cross section  $\gamma\gamma \rightarrow \pi^0\pi^0$ . The resulting  $\sigma(\gamma\gamma \rightarrow \pi^0\pi^0)$  and  $\Gamma(\sigma \rightarrow \gamma\gamma)$  are given in section 3. We elaborate our conclusions in section 4.

## 2 Dispersive approach to $\gamma\gamma \rightarrow \pi^0\pi^0$

In refs.[17, 18, 19] an interesting approach was established to calculate in terms of a dispersion relation the  $\gamma\gamma \rightarrow (\pi\pi)_I$  S-wave amplitudes,  $F_I(s)$ , where the two pions have definite isospin  $I$ . Notice that for  $\gamma\gamma \rightarrow \pi^0\pi^0$ , due to the null charge of  $\pi^0$ , there is no Born term, fig.1. One then expects, as remarked in ref.[18], that only the S-wave would be the important partial wave at low energies,  $\sqrt{s} \lesssim 0.7$  GeV. For  $\gamma\gamma \rightarrow \pi^+\pi^-$ , where there is a Born term due to the exchange of charged pions, the D-waves have a relevant contribution already at rather low energies due to the smallness of the pion mass. In the following, we shall restrict ourselves to the S-wave contribution to  $\gamma\gamma \rightarrow \pi^0\pi^0$ . The explicit calculation of ref.[10] indicates that the D-wave contribution at  $\sqrt{s} \simeq 0.65$  GeV is smaller than a 10% in  $\sigma(\gamma\gamma \rightarrow \pi^0\pi^0)$ , and it rapidly decreases for lower energies.

The function  $F_I(s)$  is an analytic function on the complex  $s$ -plane except for two cuts along the real axis. The right hand cut happens for  $s \geq 4m_\pi^2$ , with  $m_\pi$  the pion mass, and is due to unitarity. The left hand cut, in turn, runs for  $s \leq 0$  and is due to unitarity in crossed channels. Let us denote by  $L_I(s)$  the

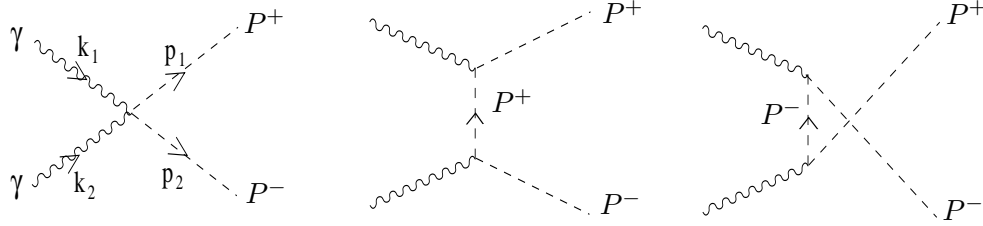


Figure 1: Born term contribution to  $\gamma(k_1)\gamma(k_2) \rightarrow P^+(p_1)P^-(p_2)$ .

complete left hand cut contribution. Then the function  $F_I(s) - L_I(s)$ , by definition, only has right hand cut. Next, refs.[17, 18, 19] consider the Omnès function  $\omega_I(s)$ ,

$$\omega_I(s) = \exp \left[ \frac{s}{\pi} \int_{4m_\pi^2}^{\infty} \frac{\phi_I(s')}{s'(s' - s)} ds' \right], \quad (2.1)$$

with  $\phi_I(s)$  the phase of  $F_I(s)$  modulo  $\pi$ , chosen in such a way that  $\phi_I(s)$  is *continuous* and  $\phi_I(4m_\pi^2) = 0$ . Because of the choice of the phase function  $\phi_I(s)$  in eq.(2.1), the function  $F_I(s)/\omega_I(s)$  has no right hand cut. Then refs.[17, 18, 19] perform a twice subtracted dispersion relation for  $(F_I(s) - L_I(s))/\omega_I(s)$ ,

$$F_I(s) = L_I(s) + a_I \omega_I(s) + c_I s \omega_I(s) + \frac{s^2}{\pi} \omega_I(s) \int_{4m_\pi^2}^{\infty} \frac{L_I(s') \sin \phi_I(s')}{s'^2(s' - s)|\omega_I(s')|} ds'. \quad (2.2)$$

On the other hand, Low's theorem [21] requires  $F_I \rightarrow B_I(s)$  for  $s \rightarrow 0$ , with  $B_I$  the Born term contribution, shown in fig.1. If we write  $L_I = B_I + R_I$ , with  $R_I \rightarrow 0$  for  $s \rightarrow 0$ , as can always be done, then Low's theorem implies also that  $F_I - L_I \rightarrow 0$  for  $s \rightarrow 0$  and hence  $a_I = 0$ .

For the exotic  $I = 2$  S-wave one can invoke Watson's final state theorem<sup>#1</sup> so that  $\phi_2(s) = \delta_\pi(s)_2$ , the  $I = 2$  S-wave  $\pi\pi$  phase shifts. For  $I = 0$  the same theorem guarantees that  $\phi_0(s) = \delta_\pi(s)_0$  for  $s \leq 4m_K^2$ , with  $\delta_\pi(s)_0$  the S-wave  $I = 0$   $\pi\pi$  phase shifts and  $m_K$  the kaon mass. Here one neglects the inelasticity due to the  $4\pi$  and  $6\pi$  states below the two kaon threshold, an accurate assumption as indicated by experiment [22, 23]. Above the two kaon threshold,  $s_K = 4m_K^2$ , the phase function  $\phi_0(s)$  cannot be fixed *a priori* due to the onset of inelasticity. This is why ref.[17] took for  $s > s_K$  that either  $\phi_0(s) \simeq \delta_\pi(s)_0$  or  $\phi_0(s) \simeq \delta_\pi(s)_0 - \pi$ , in order to study the size of the uncertainty induced for low energies. It results, however, that this uncertainty increases dramatically with energy such that for  $\sqrt{s} = 0.5, 0.55, 0.6$  and  $0.65$  GeV it is 20, 45, 92 and 200 %, see fig.3 of ref.[17].

The reason for this behaviour is the use of the function  $\omega_0(s)$  in eq.(2.2). The  $I = 0$  S-wave phase shift  $\delta_\pi(s)_0$  has a rapid increase by  $\pi$  around  $s_K = 4m_K^2$ , due to the narrowness of the  $f_0(980)$  resonance on top of the  $K\bar{K}$  threshold. Let us denote by  $\varphi(s)$  the phase of the  $\pi\pi \rightarrow \pi\pi$   $I = 0$  S-wave strong amplitude, modulo  $\pi$ , such that it is continuous and  $\varphi(4m_\pi^2) = 0$ . This phase is shown in fig.2 together with  $\delta_\pi(s)_0$  and  $\delta_\pi(s)_2$ . Now, if one uses  $\varphi(s)$  instead of  $\phi_0(s)$  in eq.(2.1) for illustration, the function  $\omega_0(s)$  is discontinuous in the transition from  $\delta_\pi(s_K)_0 \rightarrow \pi - \epsilon$  to  $\delta_\pi(s_K)_0 \rightarrow \pi + \epsilon$ , with  $\epsilon \rightarrow 0^+$ . In the first case  $|\omega_0(s)|$  has a zero at  $s_K$ , while in the latter it becomes  $+\infty$ . This discontinuity is illustrated in fig.3 by considering the difference between the dot-dashed and dashed lines. This discontinuous behaviour of  $\omega_0(s)$  under small (even tiny) changes of  $\delta_\pi(s)_0$  around  $s_K$ , was the reason for the controversy regarding the value of the pion scalar radius  $\langle r^2 \rangle_s^\pi$  between [24, 25, 26] and [27]. This controversy was finally solved

<sup>#1</sup>This theorem implies that the phase of  $F_I(s)$  where there is no inelasticity is the same, modulo  $\pi$ , as the one of the isospin  $I$  S-wave  $\pi\pi$  elastic strong amplitude.

in ref.[28] where it is shown that Ynduráin's method is compatible with the solutions obtained by solving the Muskhelishvili-Omnès equations for the scalar form factor [29, 30, 31]. The problem arose because refs.[24, 25] overlooked the proper solution and stuck to an unstable one.

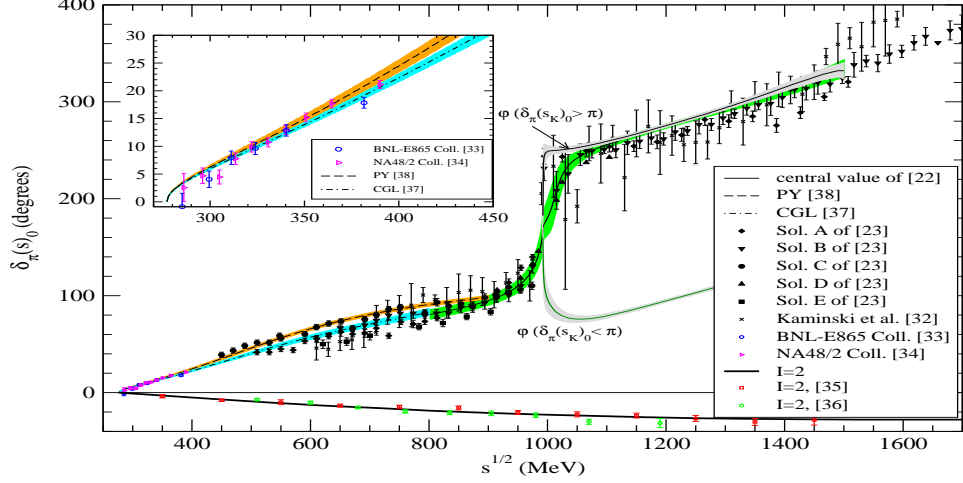


Figure 2: The phase shifts  $\delta_\pi(s)_0$  and  $\delta_\pi(s)_2$  and the phase  $\varphi(s)$ . Experimental data are from refs.[32, 23, 33, 34] for  $I = 0$  and refs.[35, 36] for  $I = 2$ . The insert is the comparison of CGL [37] and PY [38] with the accurate data from  $K_{e4}$  [33, 34].

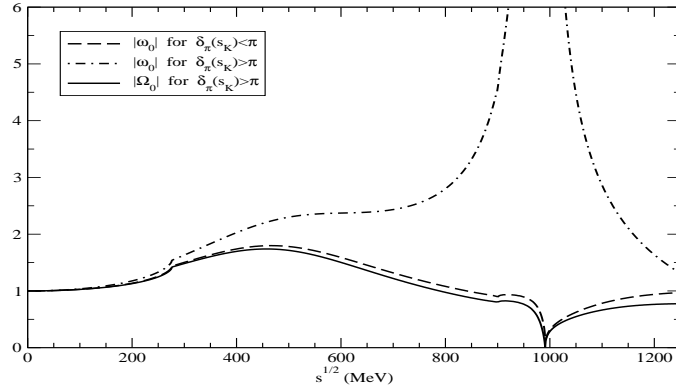


Figure 3:  $|\omega_0(s)|$ , eq.(2.1), with  $\delta_\pi(s_K)_0 < \pi$ , dashed-line, and  $\delta_\pi(s_K)_0 > \pi$ , dot-dashed line. The solid line is  $|\Omega_0(s)|$ , eq.(2.3), for the latter case. Here  $\varphi(s)$  is used as  $\phi_0(s)$  in eqs.(2.1) and (2.3) for illustrative purposes.

Inelasticity is again small for  $1.1 \lesssim \sqrt{s} \lesssim 1.5$  GeV being compatible with zero experimentally [22, 23]. As remarked in refs.[24, 28], one can then apply approximately Watson's final state theorem and for  $F_0(s)$  this implies that  $\phi_0(s) \simeq \delta^{(+)}(s)$  modulo  $\pi$ . Here  $\delta^{(+)}(s)$  is the eigenphase of the  $\pi\pi$ ,  $K\bar{K}$   $I = 0$  S-wave S-matrix such that it is continuous and  $\delta^{(+)}(s_K) = \delta_\pi(s_K)_0$ . In refs.[25, 28] it is shown that  $\delta^{(+)}(s) \simeq \delta_\pi(s)_0$  or  $\delta_\pi(s)_0 - \pi$ , depending on whether  $\delta_\pi(s_K)_0 \geq \pi$  or  $< \pi$ , respectively. In order to fix the integer factor in front of  $\pi$  in  $\phi_0(s) \simeq \delta^{(+)}(s)$  modulo  $\pi$ , one needs to devise an argument to follow the possible trajectories of  $\phi_0(s)$  in the narrow region  $1 \lesssim \sqrt{s} \lesssim 1.1$  GeV, where inelasticity is not negligible. The remarkable physical effects happening there are the appearance of the  $f_0(980)$  resonance on top of the  $K\bar{K}$  threshold and the cusp effect of the latter that induces a discontinuity at  $s_K$  in the

derivative of observables, this is clearly visible in fig.2. Between 1.05 to 1.1 GeV there are no further narrow structures and observables evolve smoothly. Approximately half of the region between 0.95 and 1.05 GeV is elastic and  $\phi_0(s) = \delta_\pi(s)_0$  (Watson's theorem), so that it rises rapidly. Above  $2m_K \simeq 1$  GeV up to 1.05 GeV the function  $\phi_0(s)$  can keep increasing with energy, as  $\delta_\pi(s)_0$  or  $\varphi(s)$  for  $\delta_\pi(s_K)_0 \geq \pi$ , and this is also always the case for the corresponding phase function of the strange scalar form factor of the pion [28]. It is also the behaviour for  $\phi_0(s)$  corresponding to the explicit calculation of ref.[10]. The other possibility is a change of sign in the slope at  $s_K$  due to the  $K\bar{K}$  cusp effect such that  $\phi_0(s)$  starts a rapid decrease in energy, like  $\varphi(s)$  for  $\delta_\pi(s_K)_0 < \pi$ , fig.2. Above  $\sqrt{s} = 1.05$  GeV,  $\phi_0(s)$  matches smoothly with the behaviour for  $\sqrt{s} \gtrsim 1.1$  GeV where it is constrained by Watson's final state theorem. As a result of this matching, for  $\sqrt{s} \gtrsim 1$  GeV *either*  $\phi_0(s) \simeq \delta_\pi(s)_0$  *or*  $\phi_0(s) \simeq \delta_\pi(s)_0 - \pi$ , corresponding to an increasing or decreasing  $\phi_0(s)$  above  $s_K$ , respectively. There is then left an ambiguity of  $\pi$  in  $\phi_0(s)$  for  $1.5 \text{ GeV} \gtrsim \sqrt{s} > \sqrt{s_K}$ . Our argument also justifies the similar choice of phases in ref.[17] above  $s_K$  to estimate uncertainties. Let us define the switch  $z$  to characterize the behaviour of  $\phi_0(s)$  for  $s > s_K$  such that  $z = +1$  if  $\phi_0(s)$  rises with energy and  $z = -1$  if it decreases. Above 1.5 GeV the phase function employed has little effect in our energy region and we use the same asymptotic phase function as in ref.[28], tending either to  $2\pi$  ( $z = +1$ ) or  $\pi$  ( $z = -1$ ) for  $s \rightarrow +\infty$ . It allows a large uncertainty of  $\simeq 2\pi$  at  $\sqrt{s} = 1.5$  GeV, that only shrinks logarithmically for higher energies. This uncertainty is included in our error analysis. Further details are given in ref.[28].

Next, we define, the function  $\Omega_0(s)$ , similarly as done in ref.[28],

$$\Omega_0(s) = \left(1 - \theta(z) \frac{s}{s_1}\right) \exp \left[ \frac{s}{\pi} \int_{4m_\pi^2}^{\infty} \frac{\phi_0(s')}{s'(s' - s)} ds' \right], \quad (2.3)$$

where  $\theta(z) = +1$  for  $z = +1$  and 0 for  $z = -1$  and  $s_1$  is the point at which  $\phi_0(s_1) = \pi$ . The latter is the only point where the imaginary part of  $\Omega_0(s)$  vanishes around  $s_K$  and this fixes the position of the zero. Now, we perform the same twice subtracted dispersion relation as in eq.(2.2) but for  $(F_0(s) - L_0(s))/\Omega_0(s)$ ,

$$F_0(s) = L_0(s) + c_0 s \Omega_0(s) + \frac{s^2}{\pi} \Omega_0(s) \int_{4m_\pi^2}^{\infty} \frac{L_0(s') \sin \bar{\phi}_0(s')}{s'^2 (s' - s) |\Omega_0(s')|} ds' + \theta(z) \frac{\omega_0(s)}{\omega_0(s_1)} \frac{s^2}{s_1^2} (F_0(s_1) - L_0(s_1)). \quad (2.4)$$

In the previous equation we introduce  $\bar{\phi}_0(s)$  that is defined as the phase of  $\Omega_0(s)$ . Let us note that in the case  $z = +1$  the phase of  $\Omega_0(s)$  for  $s > s_1$  is not  $\phi_0(s)$  but  $\phi_0(s) - \pi$ , due to the factor  $1 - (s + i\epsilon)/s_1$  in  $\Omega_0(s)$ , eq.(2.3). Since  $\phi_2(s)$ , because of Watson's final state theorem, is given by  $\delta_\pi(s)_2$ , which is small and smooth [35, 36], fig.2, the issue of the discontinuity in  $\omega_2(s)$  under changes in parameterizations does not rise and we use the dispersion relation in eq.(2.2). It is worth mentioning that our eq.(2.4) for  $z = +1$  is equivalent to take a three times subtracted dispersion relation for  $(F_0(s) - L_0(s))/\omega_0(s)$ , two subtractions are taken at  $s = 0$  and another one at  $s_1$ . We could have taken the three subtractions at  $s = 0$ , although we find more convenient eq.(2.4) which is physically motivated by the use of the Omnès function eq.(2.3) that is continuous under changes in the parameterization of the  $I = 0$  S-wave S-matrix. When eq.(2.3) is used with  $\varphi(s)$  instead of  $\phi_0(s)$  for  $\delta_\pi(s_K)_0 > \pi$  the solid curve in fig.3 is obtained, which is again close to the dashed line for  $\delta_\pi(s_K)_0 < \pi$ .

We denote by  $F_N(s)$  the S-wave  $\gamma\gamma \rightarrow \pi^0\pi^0$  amplitude and by  $F_C(s)$  the  $\gamma\gamma \rightarrow \pi^+\pi^-$  one. The relations between  $F_0$ ,  $F_2$  and  $F_N(s)$ ,  $F_C(s)$  in our isospin convention are

$$F_N(s) = -\frac{1}{\sqrt{3}}F_0 + \sqrt{\frac{2}{3}}F_2, \quad F_C(s) = -\frac{1}{\sqrt{3}}F_0 - \sqrt{\frac{1}{6}}F_2. \quad (2.5)$$

We have the unknown constants  $c_0$ ,  $c_2$  and  $F_0(s_1) - L_0(s_1)$ , the latter for  $z = +1$ . To determine them we impose:

1.  $F_C(s) - B_C(s)$  vanishes linearly in  $s$  for  $s \rightarrow 0$  and we match the coefficient to the one loop  $\chi$ PT result [4, 5].
2.  $F_N(s)$  vanishes linearly for  $s \rightarrow 0$  as well and the coefficient can be obtained again by matching with one loop  $\chi$ PT [4, 5].
3. For  $I = 0$  and  $z = +1$  one has still  $F_0(s_1) - L_0(s_1)$ . The value of this constant can be restricted taking into account that  $F_N(s)$  has an Adler zero, due to chiral symmetry. This zero is located at  $s_A = m_\pi^2$  in one loop  $\chi$ PT and moves to  $s_A = 1.175 m_\pi^2$  in two loop  $\chi$ PT [6]. This implies about a 20% correction, that prevents us from taking a definite value for  $s_A$ . In turn, we obtain that the value of the resulting cross section  $\sigma(\gamma\gamma \rightarrow \pi^0\pi^0)$  around the  $f_0(980)$  resonance is quite sensitive to the position of the Adler zero, because it controls the size of  $F_0(s_1) - L_0(s_1)$ . The latter appears in the last term in eq.(2.4), the one that dominates  $F_0(s)$  around the  $f_0(980)$  position since  $\Omega_0(s_1) = 0$ . Though the dispersive method is devised at its best for lower energies, it is also clear that it should give at least the proper order of magnitude for  $\sigma(\gamma\gamma \rightarrow \pi^0\pi^0)$  in the  $f_0(980)$  region.<sup>#2</sup> Being conservative, we shall restrict the values of  $F_0(s_1) - L_0(s_1)$  so as the cross section at  $s_1$  is less than 10 times the experimental value around the  $f_0(980)$  region,  $\sigma(\gamma\gamma \rightarrow \pi^0\pi^0) < 400$  nb.

Regarding  $L_I(s)$ , it is expected to be dominated at low energies by the Born term in isospin  $I$  because of the smallness of the pion mass. The Born term originates by the exchanges in the  $t$  and  $u$  channels ( $\gamma\pi \rightarrow \gamma\pi$ ) of charged pions, fig.1. Other crossed exchanges of vector and axial vector resonances are relatively suppressed for  $F_I(s)$  due to the larger masses of the members of the  $J^{PC} = 1^{--}, 1^{++}$  and  $1^{+-}$  multiplets so that their associated left hand cut singularities are further away. Among them, the  $1^{++}$  axial vector exchange contributions are the dominant ones in  $\gamma\pi^\pm \rightarrow \gamma\pi^\pm$  and already appear at the one loop level in  $\chi$ PT. The  $1^{--}$  and  $1^{+-}$  exchanges start one order higher. As already remarked in ref.[8], the authors of refs.[18, 19], and later on also ref.[17], overlooked the axial vector exchange contributions altogether and hence they are missing an essential part in the study of the low energy  $\gamma\gamma \rightarrow \pi^0\pi^0$ . Indeed, once the  $1^{++}$  axial vector exchange contributions are considered the cross section in the latter references would increase significantly at low energies. For instance, at  $\sqrt{s} = 0.5$  GeV one has more than a 20% increase compared to the case in which only the Born term and the  $1^{--}$  vector resonances exchanges are considered. At low energies the influence of the  $1^{+-}$  axial vector nonet is much smaller than that of the  $1^{++}$  and  $1^{--}$  multiplets. In the following,  $L_I(s)$  is modelled by the Born terms and the crossed exchanges of the  $1^{++}$ ,  $1^{--}$ , and  $1^{+-}$  resonance multiplets, evaluated from chiral Lagrangians. Explicit expressions for the distinct contributions to  $L_I(s)$  will be given elsewhere [41].

### 3 Results

In this section we show the results that follow by the use of eq.(2.4) for  $I = 0$  and eq.(2.2) for  $I = 2$ . Since the main contribution in the low energy region to  $\Omega_0(s)$  and  $\omega_2(s)$  comes from the low energy  $\pi\pi$  phase shifts, one needs to be as precise as possible for low energy  $\pi\pi$  scattering data. The small  $I = 2$  S-wave  $\pi\pi$  phase shifts, which induce small final state interaction corrections anyhow, can be parameterized in simple terms and our fit compared to data can be seen in fig.2. For the  $I = 0$  S-wave  $\pi\pi$ , we take the parameterizations of ref.[37] (CGL) and ref.[38] (PY). Both agree with data from  $K_{e4}$  decays [33, 34] and span to a large extend the band of theoretical uncertainties in the  $I = 0$  S-wave  $\pi\pi$  phase shifts [22, 23, 32]. PY, similarly to refs.[42, 43, 44], runs through the higher values of  $\delta_\pi(s)_0$ , while CGL does through lower values, see fig.2. We shall use CGL up to 0.8 GeV, since this is the upper limit of its analysis, and the K-matrix of Hyams *et al.* [22] above that energy. The latter corresponds to the energy dependent analysis of the experimental data of the same reference. On the other hand, PY is

---

<sup>#2</sup>E.g., other models [10, 39, 40] having similar physical mechanisms describe that energy region very well indeed.

used up to 0.9 GeV, since at that energy this parameterization agrees well inside errors with [22], and above 0.9 GeV the K-matrix of ref.[22] is taken. Given the input functions  $\phi_I(s)$  and  $L_I(s)$ , the constants  $c_2$ ,  $c_0$  and  $F_0(s_1) - L_0(s_1)$  can be fixed by the three conditions explained at the end of section 2. The  $\gamma\gamma \rightarrow \pi^0\pi^0$  S-wave amplitude  $F_N(s)$ , eq.(2.5), can then be calculated and the total cross section is given by  $\sigma(\gamma\gamma \rightarrow \pi^0\pi^0) = \frac{\beta}{64\pi s} |F_N(s)|^2$ , with  $\beta(s) = \sqrt{1 - 4m_\pi^2/s}$ . We show in fig.4 the drastic reduction in the uncertainty of the cross section due to the variation of  $\phi_0(s)$  above  $s_K$  as commented in the previous section. For  $z = +1$  one has the solid line while for  $z = -1$  the dashed line results, both are very close. This should be compared with the dot-dashed line that is obtained from the approach of refs.[17, 18, 19]. The uncertainty now, by employing eq.(2.4) instead of eq.(2.2) for  $I = 0$ , is drastically reduced. This improvement also implies that our results can be compared with data for  $\sqrt{s} \gtrsim 0.5$  GeV. We also show by the gray band around the solid line the mild influence in our calculations of the uncertainty in the location of the Adler zero, restricted so that  $\sigma(\gamma\gamma \rightarrow \pi^0\pi^0) < 400$  nb at the  $f_0(980)$  region (experiment is  $\simeq 40$  nb).

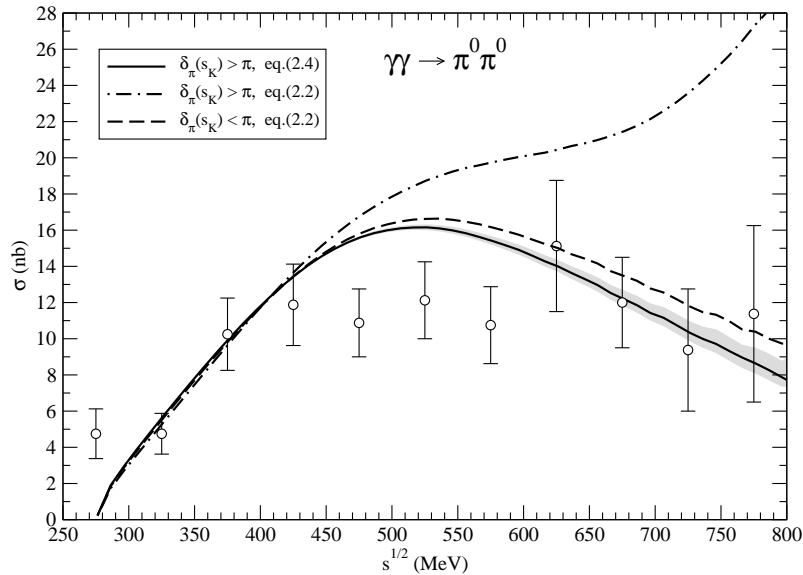


Figure 4: The solid line corresponds to  $z = +1$  and the error band is the uncertainty by requiring that  $\sigma(\gamma\gamma \rightarrow \pi^0\pi^0) < 400$  nb at  $s_1$ . This line should be compared with the dot-dashed one that would result from the formalism of ref.[17], including axial vector exchanges. Finally, the dashed line corresponds to  $z = -1$ .

Our final  $\sigma(\gamma\gamma \rightarrow \pi^0\pi^0)$  is shown in fig.5. We give the corresponding results for CGL(solid) and PY(dashed), where the band around every line stems from the uncertainties in our approach, which comprise: the errors in the Hyams *et al.* [22], CGL and PY parameterizations (those of the last two indeed dominate the width of the bands), to use either  $\phi_0(s) \simeq \delta_\pi(s)_0$  or  $\delta_\pi(s)_0 - \pi$  for  $s > s_K$ , the uncertainty in the asymptotic phase and to restrict  $\sigma(\gamma\gamma \rightarrow \pi^0\pi^0) < 400$  nb in the  $f_0(980)$  region for  $z = +1$ . On top of that, we evaluate the conditions **1** and **2** above from the expressions given by one loop  $\chi$ PT either by employing  $f_\pi = 92.4$  MeV or  $f \simeq 0.94f_\pi$ , where the former is the pion decay constant and the latter is the same but in the  $SU(2)$  chiral limit [3]. This amounts to around a 12% of uncertainty in the evaluation of  $c_0$  and  $c_2$ , due to the square dependence on  $f_\pi$ . Note that both choices,  $f_\pi$  or  $f$ , are consistent with the precision of the one loop calculation and the variation in the results is an estimate for higher order corrections. However, the error induced in  $\sigma(\gamma\gamma \rightarrow \pi^0\pi^0)$  is much smaller than that from the other sources of uncertainty and can be neglected when added in quadrature.

In the same figure the dotted line corresponds to one loop CHPT [4, 5] and the dot-dashed one to the two loop result [6, 7]. The latter is closer to our results but still one observes that the  $\mathcal{O}(p^8)$  corrections would be sizable. It is worth stressing that if the axial vector exchanges were removed, as in refs.[17, 19], then our curves would be smaller. This corresponds to the dot-dot-dashed line in fig.5 which is very close to that of ref.[17] when employing  $\phi_0(s) \simeq \delta_\pi(s)_0 - \pi$  for  $s > s_K$ . This curve is evaluated making use of CGL and ref.[22]. The three experimental points [1] in the region  $0.45 - 0.6$  GeV agree well with this curve. However, once the axial vector are included the curve rises. These three points lie around 1.5 sigmas below the CGL result band, and by more than two sigmas below the PY one. This clearly shows that more precise experimental data on  $\gamma\gamma \rightarrow \pi^0\pi^0$  could be used to distinguish between different S-wave parameterizations. In turn, the next three experimental  $\sigma(\gamma\gamma \rightarrow \pi^0\pi^0)$  points, those lying between  $0.6 - 0.75$  GeV, agree better when the axial vector resonance contributions are taken into account, as one should do. As a result of this discussion, more precise experimental data for  $\gamma\gamma \rightarrow \pi^0\pi^0$  are called for.

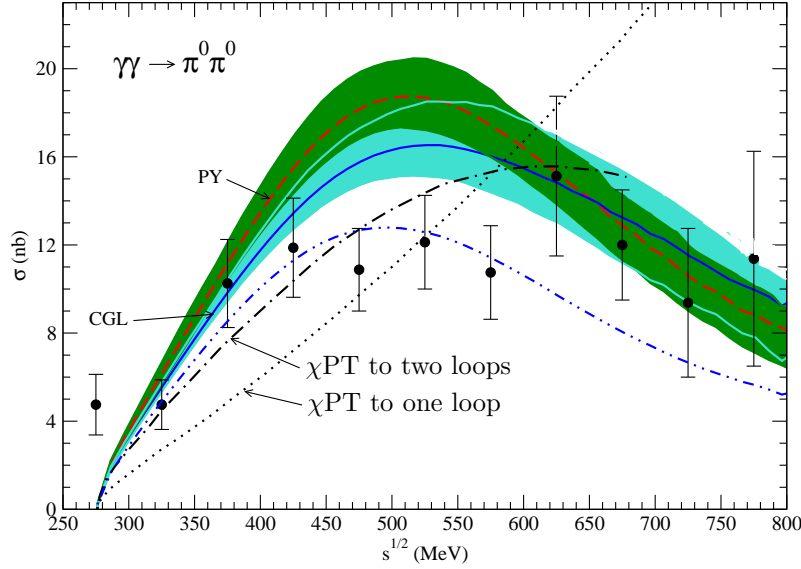


Figure 5: Final results for the  $\gamma\gamma \rightarrow \pi^0\pi^0$  cross section. Experimental data are from the Crystal Ball Coll. [1], scaled by  $1/0.8$ , as  $|\cos\theta| < 0.8$  is measured and S-wave dominates. The solid line corresponds to CGL and the dashed one to PY. The dot-dot-dashed line results after removing the axial vector exchange contributions. The band along each line represents the theoretical uncertainty. The dotted line is the one loop  $\chi$ PT result [4, 5] and the dot-dashed one the two loop calculation [6].

In terms of the calculated  $F_N(s)$  one can evaluate the  $\sigma$  coupling to  $\gamma\gamma$ , called  $g_{\sigma\gamma\gamma}$ . The dispersion relation to calculate  $F_0(s)$  is only valid on the first Riemann sheet. If evaluated on the second Riemann sheet there would be an extra term due to the  $\sigma$  pole. However, the relation between  $F_0(s)$  and  $\tilde{F}_0(s)$ , the latter on the second sheet, can be easily established by using unitarity above the  $\pi\pi$  threshold,

$$F_0(s+i\epsilon) - F_0(s-i\epsilon) = -2iF_0(s+i\epsilon)\rho(s+i\epsilon)T_{II}^0(s-i\epsilon), \quad (3.6)$$

with  $4m_\pi^2 \leq s \leq 4m_K^2$ ,  $\rho(s) = \beta(s)/16\pi$  and  $\epsilon \rightarrow 0^+$ . In the equation above  $T_{II}^0(s)$  is the  $I=0$  S-wave  $\pi\pi$  elastic amplitude on the second Riemann sheet and  $T_I^0(s)$  is the one on the physical Riemann sheet. Due to continuity when changing from one sheet to the other,  $F_0(s-i\epsilon) = \tilde{F}_0(s+i\epsilon)$ ,  $T_I^{I=0}(s-i\epsilon) = T_{II}^{I=0}(s+i\epsilon)$ . Then, eq.(3.6) can be rewritten as

$$\tilde{F}_0(s) = F_0(s) (1 + 2i\rho(s)T_{II}^{I=0}(s)). \quad (3.7)$$



Around the  $\sigma$  pole,  $s_\sigma$ ,

$$T_{II}^{I=0} = \frac{g_{\sigma\pi\pi}^2}{s_\sigma - s}, \quad \tilde{F}_0(s) = \sqrt{2} \frac{g_{\sigma\gamma\gamma} g_{\sigma\pi\pi}}{s_\sigma - s}, \quad (3.8)$$

with  $g_{\sigma\pi\pi}$  the  $\sigma$  coupling to two pions such that  $\Gamma = |g_{\sigma\pi\pi}|^2 \beta / 16\pi M$ , for a narrow enough scalar resonance of mass  $M$ . Notice as well the  $\sqrt{2}$  factor in  $\tilde{F}_0(s)$  to match with the  $g_{\sigma\pi\pi}$  normalization used (the so called unitary normalization [42, 43, 44]). Then from eqs.(3.7) and (3.8) it follows that

$$\frac{g_{\sigma\gamma\gamma}^2}{g_{\sigma\pi\pi}^2} = -\frac{1}{2} \left( \frac{\beta(s_\sigma)}{8\pi} \right)^2 F_0(s_\sigma)^2, \quad (3.9)$$

Let us stress that this equation gives the ratio between the residua of the S-wave  $I = 0$   $\gamma\gamma \rightarrow \pi\pi$  and  $\pi\pi \rightarrow \pi\pi$  amplitudes at the  $\sigma$  pole position.

In order to derive specific numbers for the previous ratio in terms of our dispersive approach one needs to introduce  $s_\sigma$ . We take two different values for  $s_\sigma = (M_\sigma - i\Gamma_\sigma/2)^2$ . From the studies of Unitary  $\chi$ PT [42, 43, 44, 45] one has  $M_\sigma$  and  $\Gamma_\sigma$  around the interval 425-440 MeV. The other values that we will use are from ref. [46],  $M_\sigma^{ccl} = 441_{-8}^{+16}$  MeV and  $\Gamma_\sigma^{ccl} = 544_{-25}^{+18}$  MeV, where the superscript *ccl* indicates, in the following, values that employ the  $\sigma$  pole position of ref.[46]. The corresponding ratios of the residua given in eq.(3.9) are:

$$\begin{aligned} \left| \frac{g_{\sigma\gamma\gamma}}{g_{\sigma\pi\pi}} \right| &= (2.10 \pm 0.25) \times 10^{-3}, \quad s_\sigma \text{ from ref. [45]}, \\ \left| \frac{g_{\sigma\gamma\gamma}}{g_{\sigma\pi\pi}} \right| &= (2.06 \pm 0.14) \times 10^{-3}, \quad s_\sigma \text{ from ref. [46]}. \end{aligned} \quad (3.10)$$

Both numbers are very similar despite that the imaginary parts of the two  $s_\sigma^{1/2}$  differ by  $\sim 20\%$ . The result of [17], with which we shall compare our results later, corresponds to the ratio in eq.(3.10) being 20% bigger at  $(2.53 \pm 0.09) \times 10^{-3}$  with  $s_\sigma$  of ref.[46].

These ratios of residua at the  $\sigma$  pole position are the well defined predictions that follow from our improved dispersive treatment of  $\gamma\gamma \rightarrow (\pi\pi)_I$ . However, the radiative width to  $\gamma\gamma$  for a wide resonance like the  $\sigma$ , though more intuitive, has experimental determinations that are parameterization dependent. This is due to the non-trivial interplay between background and the broad resonant signal. An unambiguous definition is then required [17, 19]. We employ, as in ref.[17], the standard narrow resonance width formula in terms of  $g_{\sigma\gamma\gamma}$  determined from eq.(3.9) by calculating the residue at  $s_\sigma$ ,

$$\Gamma(\sigma \rightarrow \gamma\gamma) = \frac{|g_{\sigma\gamma\gamma}|^2}{16\pi M_\sigma}. \quad (3.11)$$

Nevertheless, the determinations of the radiative widths from this expression and those from common experimental analyses can differ substantially. The following example makes this point clear.

From ref.[45] one obtains  $|g_{\sigma\pi\pi}| = 2.97 - 3.01$  GeV, corresponding to the square root of the residua of the  $I = 0$  S-wave  $\pi\pi$  amplitude, as in eq.(3.8). If similarly to eq.(3.11), one uses the formula,

$$\Gamma_\sigma = \frac{|g_{\sigma\pi\pi}|^2 \beta(M_\sigma)}{16\pi M_\sigma}, \quad (3.12)$$

the resulting width lies in the range 309 – 319 MeV, that is around a 30% smaller than  $\Gamma_\sigma \simeq 430$  MeV from the pole position of ref.[45]. This is due to the large width of the  $\sigma$  meson which makes the  $|g_{\sigma\pi\pi}|$  extracted from the residue of  $T_{II}^{I=0}$ , eq.(3.8), be smaller by around a 15% than the value needed in

eq.(3.12) to obtain  $\Gamma_\sigma \simeq 430$  MeV. Similar effects are then also expected in order to extract  $\Gamma(\sigma \rightarrow \gamma\gamma)$  from the eq.(3.11). Equations similar to this are usually employed in phenomenological fits to data, e.g. see ref.[47], but with  $|g_{\sigma\gamma\gamma}|$  determined along the real axis. As a result of this discussion, one should allow a (20–30)% variation between the results obtained from eq.(3.11) and those from standard experimental analyses that still could deliver a  $\gamma\gamma \rightarrow \pi\pi$  amplitude in agreement with our more theoretical treatment for physical values of  $s$ .

We shall employ the following values for  $|g_{\sigma\pi\pi}|$ . First we take  $|g_{\sigma\pi\pi}| = 2.97 - 3.01$  GeV [42, 43, 44, 45]. With this value the resulting two photon width from eqs.(3.10) and (3.11) is

$$\Gamma(\sigma \rightarrow \gamma\gamma) = (1.8 \pm 0.4) \text{ KeV} . \quad (3.13)$$

We also consider a larger value for  $|g_{\sigma\pi\pi}|$  since  $\Gamma_\sigma^{ccl}$  [46] is larger by a factor  $\sim 1.3$  than  $\Gamma_\sigma$  from ref.[45]. One value is

$$|g_{\sigma\pi\pi}|_{(1)}^{ccl} \simeq |g_{\sigma\pi\pi}| \left( \frac{\Gamma_\sigma^{ccl}(\sigma \rightarrow \pi\pi)}{\Gamma(\sigma \rightarrow \pi\pi)} \right)^{\frac{1}{2}} = (1.127 \pm 0.022) |g_{\sigma\pi\pi}| = (3.35 \pm 0.08) \text{ GeV} . \quad (3.14)$$

This corresponds to the scenario discussed previously in eq.(3.12) with a value 15% lower than

$$|g_{\sigma\pi\pi}|_{(2)}^{ccl} = \left( \frac{16\pi M_\sigma \Gamma_\sigma^{ccl}}{\beta(M_\sigma)} \right)^{1/2} = (3.93 \pm 0.08) \text{ GeV} , \quad (3.15)$$

obtained by reproducing  $\Gamma_\sigma^{ccl}$  from the pole position using eq.(3.12). If we evaluate with these couplings the  $\sigma \rightarrow \gamma\gamma$  width one obtains from eqs.(3.10) and (3.11), respectively,

$$\begin{aligned} \Gamma_{(1)}^{ccl}(\sigma \rightarrow \gamma\gamma) &= (2.1 \pm 0.3) \text{ KeV} , \\ \Gamma_{(2)}^{ccl}(\sigma \rightarrow \gamma\gamma) &= (3.0 \pm 0.3) \text{ KeV} . \end{aligned} \quad (3.16)$$

Recently, ref.[17] calculated a value  $\Gamma(\sigma \rightarrow \gamma\gamma) = (4.09 \pm 0.29) \text{ KeV}$  also employing  $s_\sigma$  from ref.[46]. This value is larger than  $\Gamma_{(2)}^{ccl}(\sigma \rightarrow \gamma\gamma)$  in the previous equation, despite that  $|g_{\sigma\pi\pi}|$  there used is 3.86 GeV, very close to  $|g_{\sigma\pi\pi}|_{(2)}^{ccl}$ . It is worth stressing that both our eq.(3.11) and eq.(7) of ref.[17] are equivalent for calculating  $\Gamma(\sigma \rightarrow \gamma\gamma)$ , except for an extra factor  $|\beta(s_\sigma)| \sim 0.95$  in ref.[17]. Of course, they are written in a different notation.<sup>#3</sup> The reason for this remaining difference is two fold. As already mentioned above, ref.[17] does not include axial vector exchanges in evaluating  $\gamma\gamma \rightarrow (\pi\pi)_I$ . It is this omission that accounts for half of the 20% difference in the ratio of residua, eq.(3.10), mentioned above. The other 10% comes from improvements delivered by our extra subtraction and our slightly different inputs. Using the same value for  $|g_{\sigma\pi\pi}|$  as in [17], our resulting value for  $\Gamma(\sigma \rightarrow \gamma\gamma)$  would be around a 40% smaller (as in eq.(3.16)) than that in [17].

As a summary of the  $\sigma \rightarrow \gamma\gamma$  considerations, from our dispersive approach and  $s_\sigma$  of refs.[45, 46] we obtain a value for the ratio of the residua  $|g_{\sigma\gamma\gamma}/g_{\sigma\pi\pi}| \sim (2.1 \pm 0.25) \times 10^{-3}$ . This number follows unambiguously from our study. Other more intuitive, but convention dependent quantities, like the  $\sigma \rightarrow \gamma\gamma$  width calculated from eq.(3.11), are less well determined. These depend critically on the input value for  $|g_{\sigma\pi\pi}|^2$  and  $s_\sigma$ , though they are not required in our dispersive study of  $\gamma\gamma \rightarrow \pi^0\pi^0$ . We then determine the values: i)  $\Gamma(\sigma \rightarrow \gamma\gamma) = (1.8 \pm 0.4) \text{ KeV}$  with  $s_\sigma$  and  $|g_{\sigma\pi\pi}| \sim 3$  GeV from ref.[45]; ii)  $\Gamma_{(1)}^{ccl}(\sigma \rightarrow \gamma\gamma) = (2.1 \pm 0.3) \text{ KeV}$  and  $\Gamma_{(2)}^{ccl}(\sigma \rightarrow \gamma\gamma) = (3.0 \pm 0.3) \text{ KeV}$  which come by considering  $s_\sigma$  of ref.[46] with an estimated  $|g_{\sigma\pi\pi}| = 3.4$  and 3.9 GeV, respectively. Other values could be obtained from eq.(3.11) by plugging different  $s_\sigma$  and  $|g_{\sigma\pi\pi}|$  in eq.(3.9) in order to estimate  $|g_{\sigma\gamma\gamma}|$ . One should require that these values are provided from a  $\pi\pi$  S-wave  $I = 0$  strong amplitude in agreement with the experimental phase shifts, see fig.2.

<sup>#3</sup>We want to thank M.R. Pennington for a detailed comparison of his results with ours and interesting discussions.

## 4 Conclusions

We have undertaken a dispersive study of the  $\gamma\gamma \rightarrow \pi^0\pi^0$  reaction. Our approach is based on that of refs.[18, 19, 17] but using a better behaved Omnès function for the  $I = 0$  S-wave  $\pi\pi$  channel. As a result, we have been able to reduce drastically the uncertainty regarding the  $\phi_0(s)$  used in this Omnès function above the  $K\bar{K}$  threshold. Our improvement is equivalent to take three subtractions instead of the two originally proposed in refs.[18, 19, 17]. We have then used two low energy conditions and a third constraint in the form of a bound on the  $f_0(980)$  region so as to fix the three subtraction constants. This has allowed us to present more accurate results, which might be used to discriminate between different  $\pi\pi$   $I = 0$  S-wave parametrizations, once more precise data on  $\sigma(\gamma\gamma \rightarrow \pi^0\pi^0)$  become available. Further improvements at the theoretical level rest on a more precise determination of  $\phi_0(s)$  above  $s_K$  and a more systematic calculation of  $L_I(s)$ .

We have calculated the ratio of the residua  $|g_{\sigma\gamma\gamma}/g_{\sigma\pi\pi}| = (2.1 \pm 0.25) \times 10^{-3}$  with  $s_\sigma$  from refs.[45, 46]. The  $\sigma$  width to  $\gamma\gamma$  was also studied and we stressed its dependence on the  $s_\sigma$  and  $|g_{\sigma\pi\pi}|^2$  employed, not used in our dispersive study of  $\gamma\gamma \rightarrow \pi^0\pi^0$ . One value obtained is  $\Gamma(\sigma \rightarrow \gamma\gamma) = (1.8 \pm 0.4)$  KeV with  $s_\sigma$  and  $|g_{\sigma\pi\pi}| \simeq 3$  GeV from ref.[45]. The others values take  $s_\sigma$  as given in ref.[46] with  $\Gamma(\sigma \rightarrow \gamma\gamma) = (2.1 \pm 0.3)$  KeV for  $|g_{\sigma\pi\pi}| = 3.4$  GeV, and  $\Gamma(\sigma \rightarrow \gamma\gamma) = (3.0 \pm 0.3)$  KeV for  $|g_{\sigma\pi\pi}| = 3.9$  GeV. The last two numbers for  $\Gamma^{ccl}(\sigma \rightarrow \gamma\gamma)$  tell us that the uncertainties in its calculation are still rather large and a further improvement requires to know precisely  $|g_{\sigma\pi\pi}^{ccl}|$  from ref.[37].

## Acknowledgements

We would like to thank E. Oset for useful communications. This work has been supported in part by the MEC (Spain) and FEDER (EC) Grants FPA2004-03470 and Fis2006-03438, the Fundación Séneca (Murcia) grant Ref. 02975/PI/05, the European Commission (EC) RTN Network EURIDICE Contract No. HPRN-CT2002-00311 and the HadronPhysics I3 Project (EC) Contract No RII3-CT-2004-506078. C.S. acknowledges the Fundación Séneca by funding his stay at the Departamento de Física de la Universidad de Murcia, and the latter by its warm hospitality.

## References

- [1] H. Marsiske *et al.* [Crystal Ball Collaboration], Phys. Rev. **D41**, 3324 (1990).
- [2] S. Weinberg, Physica **A96**, 327 (1979).
- [3] J. Gasser and H. Leutwyler, Ann. Phys. (N.Y.) **158**, 142 (1984); Nucl. Phys. **B250**, 465 (1985).
- [4] J. Bijnens and F. Cornet, Nucl. Phys. **B296**, 557 (1988).
- [5] J. F. Donoghue, B. R. Holstein and Y. C. Lin, Phys. Rev. **D37**, 2423 (1988).
- [6] S. Bellucci, J. Gasser and M. E. Sainio, Nucl. Phys. **B423**, 80 (1994).
- [7] J. Gasser, M. A. Ivanov and M. E. Sainio, Nucl. Phys. **B728**, 31 (2005).
- [8] J. F. Donoghue and B. Holstein, Phys. Rev. **D48**, 137 (1993).
- [9] A. Dobado and J. R. Peláez, Z. Phys. **C57**, 501 (1993).
- [10] J. A. Oller and E. Oset, Nucl. Phys. **A629**, 739 (1998).
- [11] J. A. Oller, Phys. Lett. **B426**, 7 (1998).
- [12] T. S. H. Lee, J. A. Oller, E. Oset and A. Ramos, Nucl. Phys. **A643** (1998) 402.
- [13] U. G. Meissner and J. A. Oller, Nucl. Phys. A **679**, 671 (2001).

- [14] J. A. Oller, E. Oset and J. E. Palomar, Phys. Rev. **D63** (2001) 114009.
- [15] E. Oset, J. A. Oller and U. G. Meissner, Eur. Phys. J. **A12**, 435 (2001).
- [16] E. Oset, J. R. Peláez and L. Roca, Phys. Rev. **D67**, 073013 (2003).
- [17] M. R. Pennington, Phys. Rev. Lett. **97** (2006) 011601.
- [18] D. Morgan and M. R. Pennington, Z. Phys. **C37**, 431 (1988); (E)-ibid. **C39**, 590 (1988); Phys. Lett. **B272**, 134 (1991).
- [19] M. R. Pennington, pag.18 in L. Maiani, G. Panchieri and N. Paver, eds., The DAΦNE Physics Handbook (INFN, Frascati, 1992).
- [20] J. Babcock and J. L. Rosner, Phys. Rev. **D14** (1976) 1286; S. Godfrey and N. Isgur, Phys. Rev. **D32** (1985) 189; T. Barnes, Phys. Lett. **B165**, 434 (1985); S. Narison and G. Veneziano, Int. J. Mod. Phys. **A4** (1989) 2751; Z. P. Li, F. E. Close and T. Barnes, Phys. Rev. **D43** (1991) 2161; C. R. Munz, Nucl. Phys. **A609** (1996) 364; N. N. Achasov, Phys. Atom. Nucl. **65** (2002) 546 [Yad. Fiz. **65**, 573 (2002)]; S. Krewald, R. H. Lemmer and F. P. Sassen, Phys. Rev. D **69** (2004) 016003; S. Rodriguez and M. Napsuciale, Phys. Rev. **D71**, 074008 (2005); C. Hanhart, Yu. S. Kalashnikova, A. E. Kudryavtsev and A. V. Nefediev, Phys. Rev. **D75** (2007) 074015; G. Mennessier, P. Minkowski, S. Narison and W. Ochs, arXiv:hep-ph/0707.4511.
- [21] F. E. Low, Phys. Rev. **96**, 1428 (1954); M. Gell-Mann and M. L. Goldberger, Phys. Rev. **96**, 1433 (1954).
- [22] B. Hyams *et al.*, Nucl. Phys. **B64**, 134 (1973).
- [23] G. Grayer *et al.*, Nucl. Phys. B **75** (1974) 189.
- [24] F. J. Ynduráin, Phys. Lett. **B578**, 99 (2004); (E)-*ibid* **B586**, 439 (2004).
- [25] F. J. Ynduráin, Phys. Lett. **B612**, 245 (2005).
- [26] F. J. Ynduráin, arXiv:hep-ph/0510317.
- [27] B. Ananthanarayan, I. Caprini, G. Colangelo, J. Gasser and H. Leutwyler, Phys. Lett. **B602**, 218 (2004).
- [28] J. A. Oller and L. Roca, Phys. Lett. **B651**, 139 (2007).
- [29] J. F. Donoghue, J. Gasser and H. Leutwyler, Nucl. Phys. **B343**, 341 (1990).
- [30] B. Moussallam, Eur. Phys. J. **C14**, 111 (2000).
- [31] U. G. Meißner and J. A. Oller, Nucl. Phys. **A679**, 671 (2001).
- [32] R. Kaminski, L. Lesniak and K. Rybicki, Z. Phys. C **74**, 79 (1997).
- [33] S Pislak *et al.* [BNL-E865 Collaboration], Phys. Rev. Lett. **87**, 221801; Phys. Rev. **D67**, 072004 (2003).
- [34] L. Masetti [NA48/2 Collaboration], arXiv:hep-ex/0610071.
- [35] M. J. Losty *et al.*, Nucl. Phys. **B69** (1974) 185.
- [36] W. Hoogland *et al.*, Nucl. Phys. **B126** (1977) 109.
- [37] G. Colangelo, J. Gasser and H. Leutwyler, Nucl. Phys. **B603**, 125 (2001).
- [38] J. R. Peláez and F. J. Ynduráin, Phys. Rev. **D68**, 074005 (2003); Phys. Rev. **D71**, 074016 (2005).
- [39] N. N. Achasov, *Proceedings of the 14th International Seminar on High Energy Physics: Quarks 2006, St. Petersburg, Russia*.
- [40] G. Mennessier, Z. Phys. **C16**, 241 (1983).
- [41] J. A. Oller, L. Roca and C. Schat, in preparation.

- [42] J. A. Oller and E. Oset, Nucl. Phys. **A620**, 438 (1997); (E)-ibid. **A652** (1999) 407.
- [43] J. A. Oller and E. Oset, Phys. Rev. **D60**, 074023 (1999).
- [44] A. Dobado and J. R. Peláez, Phys. Rev. **D56**, 3057 (1997); J. A. Oller, E. Oset and J. R. Peláez, Phys. Rev. Lett. **80**, 3452 (1998); J. A. Oller, E. Oset and J. R. Peláez, Phys. Rev. **D59**, 074001 (1999); (E)-ibid. **D60**, 099906 (1999), **D75**, 099903 (2007).
- [45] J. A. Oller, Nucl. Phys. **A727** (2003) 353.
- [46] I. Caprini, G. Colangelo and H. Leutwyler, Phys. Rev. Lett. **96** (2006) 132001.
- [47] T. Mori *et al.* [Belle Collaboration], Phys. Rev. **D75** (2007) 051101.